

A simplified mathematical approach for the evaluation of the stabilizing forces applied by a passive cemented bolt to a sliding rock block

*Original*

A simplified mathematical approach for the evaluation of the stabilizing forces applied by a passive cemented bolt to a sliding rock block / Oreste, P.; Spagnoli, G.. - In: TUNNELLING AND UNDERGROUND SPACE TECHNOLOGY. - ISSN 0886-7798. - STAMPA. - 103:(2020), p. 103459. [10.1016/j.tust.2020.103459]

*Availability:*

This version is available at: 11583/2940996 since: 2021-11-28T20:47:45Z

*Publisher:*

Elsevier Ltd

*Published*

DOI:10.1016/j.tust.2020.103459

*Terms of use:*

This article is made available under terms and conditions as specified in the corresponding bibliographic description in the repository

*Publisher copyright*

(Article begins on next page)

1 **A simplified *mathematical* approach for the evaluation of the stabilizing forces**  
2 **applied by a passive cemented bolt to a sliding rock block**

3 Pierpaolo Oreste<sup>1</sup>, Giovanni Spagnoli<sup>2\*</sup>

4 <sup>1</sup> Department of Environmental, Land and Infrastructure Engineering, Politecnico di  
5 Torino, Corso Duca Degli Abruzzi 24, 10129 Torino, Italy, *pierpaolo.oreste@polito.it*

6 ORCID: 0000-0001-8227-9807

7 <sup>2</sup> BASF Construction Solutions GmbH, Dr-Albert-Frank-Strasse 32, 83308 Trostberg,  
8 Germany, \*corresponding author, Tel: +49 8621 86-3702,

9 *giovanni.spagnoli@basf.com* ORCID: 0000-0002-1866-4345

10 **Abstract**

11 *Passive bolting is used to stabilise unstable rock blocks in surface and underground*  
12 *structures due to the various advantages it offers.* Despite its *use*, the design phase  
13 still presents aspects of considerable complexity *because* the fact that the load of the  
14 bolt and therefore, its static action *depends on its* interaction with the block and the  
15 stable rock. In the present work, a mathematical model *was* developed which is  
16 capable of directly calculating the stabilisation forces as a function of the characteristic  
17 parameters of the bolt and of *its* interaction with the rock. This discussion is based on  
18 *a simplified hypothesis of bolt behaviour, which provides negligible errors, and on the*  
19 *observation that the critical point* is positioned at the intersection of the bolt with one  
20 of the lateral surfaces that separate it from the portion of stable rock. The formulation  
21 of the stabilisation forces obtained made it possible to evaluate the static contribution  
22 of each single bolt to the stability of the rock block, by varying the diameter of the steel  
23 bar and then designing the bolting operation to achieve acceptable stability conditions

24 for the rock block. The application of **stabilising** equations to a real case, for which the  
25 results of load tests on bolt tests were available, allowed us to outline steps to be taken  
26 in the bolt design process.

27

28 **Keywords:** rock bolt; Winkler spring approach; rock block stabilisation; safety factor;  
29 bolt-rock relative displacement.

30

31 **Abbreviations and nomenclature**

32	$A_{bar}$	Area of the section of the steel bar constituting the bolt
33	$(EA)_{bolt}$	Axial stiffness of the bolt
34	$(EA)_{bolt,test}$	Axial stiffness of the tested bolt
35	$E_{binder}$	Elastic modulus of the binder surrounding the steel bar in the hole
36	$(EJ)_{bolt}$	Bending stiffness of the bolt
37	$(EJ)_{bolt,test}$	Bending stiffness of the tested bolt
38	$E_{st}$	Steel elastic modulus
39	$F_{s,yield}$	Safety factor of the bolt with respect to the tensile failure of the steel bar
40	$F_{s,slip}$	Safety factor of the failure of the bolt-rock interface due to the bolt sliding
41	$H_{1,I}$	Integration constant in the axial rock-bolt interaction
42	$H_{2,I}$	Integration constant in the axial rock-bolt interaction
43	$H_{1,II}$	Integration constant in the axial rock-bolt interaction
44	$H_{2,II}$	Integration constant in the axial rock-bolt interaction
45	$J_{bar}$	Moment of inertia of the steel bar constituting the bolt
46	$k$	Ratio between the normal pressure, $p$ , which is applied on the perimeter
47		of the bolt (on the wall of the hole) by the surrounding rock and the
48		normal displacements, $y$ , of the bolt
49	$L_a$	Bolt length inside the unstable block
50	$L_p$	Bolt length in the stable rock behind the unstable block
51	$L_{test}$	Length of the tested bolt
52	$M$	Bending moment in the bolt
53	$N$	Axial force in the bolt
54	$N_{0,max}$	Bolt stabilising force in the direction of the bolt axis

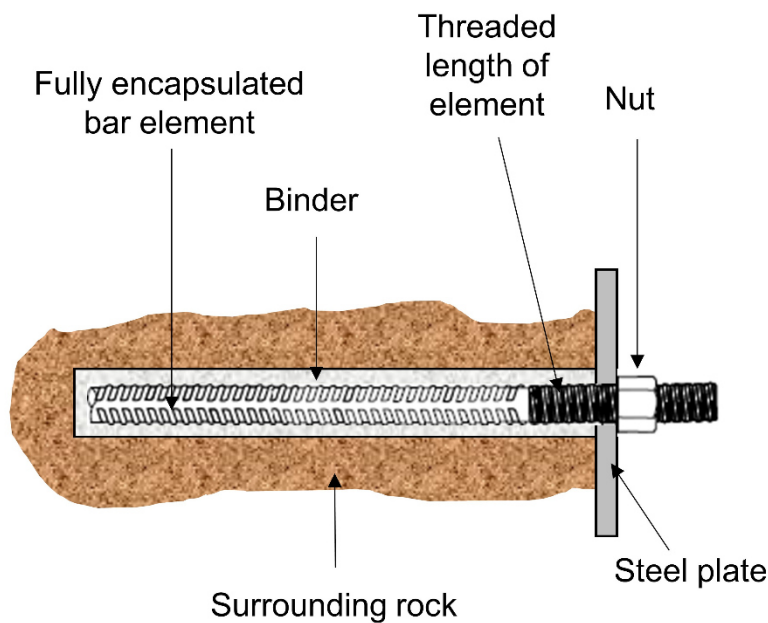
55	$N_{test}$	Tensile axial force applied at the bolt head from pull-out tests
56	$N_{yield}$	Force causing the bar failure under tensile stress
57	$N_{slip}$	Force <b>causing</b> the bolt-rock interface to fail for a unit bolt length
58	$N_{slip,test}$	Force <b>causing</b> the bolt-rock interface of the test bolt to fail (i.e., bolt slips
59		away)
60	$N_0$	Value of the tensile force in the axial direction of the bolt on the
61		intersection point between the bolt and a block surface
62	$p$	Value of the normal pressure (perpendicular to the axial direction)
63		applied on the lateral surface of the bolt
64	$P_{hole}$	Perimeter of the cross-section of the bolt
65	$P_{hole,test}$	Perimeter of the cross-section of the tested bolt
66	$S_{bar}$	Static moment of the half section of the bar with respect to the
67		barycentric axis
68	$T$	Shear force in the bolt
69	$t_{binder}$	Thickness of the binder annulus surrounding the steel bar
70	$T_0$	Value of the shear force perpendicular to the axial direction of the bolt
71		on the intersection point between the bolt and a block surface
72	$T_{0,max}$	Bolt stabilising force in the <b>transverse</b> direction
73	$T_{test}$	Force perpendicular to the axis of the bolt in correspondence to its head
74		from lateral shear tests
75	$v_r$	Value of the relative axial displacement between the bolt and the
76		surrounding rock
77	$y$	Normal displacements of the bolt perpendicular to the axial direction of
78		the bolt

79	$\alpha$	Parameter characterising the interaction in the axial direction between
80		the bolt and the surrounding rock $\alpha = \sqrt{\frac{\beta_c \cdot P_{hole}}{EA}}$
81	$\beta$	Parameter characterising the interaction in the <b>transverse</b> direction
82		between the bolt and the surrounding rock $\beta = \sqrt[4]{\frac{k \cdot \Phi_{hole}}{4 \cdot EJ}}$
83	$\beta_c$	Ratio between the shear stresses, $\tau$ , that develop on the perimeter of the
84		bolt and the relative axial displacements, $v_r$ .
85	$\delta$	Arbitrary displacement of the block
86	$\delta_n$	Displacement component of the block in the axial direction of the bolt
87	$\delta_{n,test}$	Bolt head axial displacement due to the application of the axial force,
88		$N_{test}$
89	$\delta_t$	Displacement component of the block in the <b>transverse</b> direction of the
90		bolt
91	$\delta_{t,test}$	<b>Transverse</b> bolt head displacement due to the application of a shear
92		force, $T_{test}$
93	$\Phi_{bar}$	Diameter of the steel bar
94	$\Phi_{hole}$	Diameter of the hole (of the bolt)
95	$\Phi_{hole,test}$	Diameter of the tested bolt
96	$\chi$	Adimensional parameter for the evaluation of the stabilising forces
97	$\lambda$	Adimensional parameter for the evaluation of the stabilising forces
98	$\eta$	Adimensional parameter for the evaluation of the stabilising forces
99	$\omega$	Adimensional parameter for the evaluation of the stabilising forces
100	$\psi$	Adimensional parameter for the evaluation of the stabilising forces
101	$\varrho$	Adimensional parameter for the evaluation of the stabilising forces
102	$\sigma_{yield}$	Steel yield stress

103	$\sigma_{id}$	Ideal stress which accounts for the simultaneous presence of an axial
104		and a shear stress in the same section of the steel bar
105	$\tau$	Shear stress on the lateral surface of the bolt
106	$\tau_{lim}$	Ultimate limit shear stress of the rock-bolt <b>interface</b>
107	$\tau_{0,I}$	Existing shear stress for $x=0$ (at the intersection with a lateral surface of
108		the rock block) on the side of the potentially unstable rock block
109	$\tau_{0,II}$	Existing shear stress for $x=0$ (at the intersection with a lateral surface of
110		the rock block) on the side of the portion of stable rock
111	$\xi$	Adimensional parameter for the evaluation of the stabilising forces
112		
113		

114 **Introduction**

115           Passive rock bolts (Fig. 1), which have zero initial load, are normally used to  
116 prevent rock blocks from falling or sliding. The mobilised stabilising load increases with  
117 the displacement of the potentially unstable rock block. Among the different types of  
118 passive rock anchors, fully-grouted rock bolts which rely on a binder that fills the  
119 annulus between the element and the borehole wall (Bawden, 2011) are normally used  
120 in practice and are able to support tensile, compressive, shear, and bending loads  
121 (Ghadimi et al. 2015).



122

123 **Fig. 1 Sketch of a passive rock bolt.**

124           As a result of the rock bolt deformation, a normal and a shear force act on the  
125 rock mass and restrain further deformation of the rock, transferring loads from the  
126 stable to the unstable rock mass (Nie et al. 2014). Rock bolts are used in both low and  
127 high in situ stress conditions (Li, 2017). In heavily jointed rocks, they create a  
128 ‘reinforced arch’ around an underground opening, thereby providing stability to the  
129 cavity (Lang, 1961) as the bolt action increases due to an increase in axial shear forces

130 and bending moments in the bolt rod (e.g., ; Oreste, 2009; Oreste and Dias 2012;  
131 Ranjbarnia et al., 2014, 2016). Rock bolts improve the stiffness of rocks (Chappell,  
132 1989). The main factors affecting the shear strength of rock bolts are the materials  
133 they are made of, the size of the rod body, and the type of rock mass (Ferrero, 1995).

134 Several analytical and numerical methods are found in the literature describing  
135 complex bolt-grout-rock interactions and suggesting improvements to bolt geometry,  
136 grout properties, or the interaction between the two (e.g., Blümel et al. 1997; Aziz and  
137 Jalalifar 2007; Osgoui and Oreste 2007; Das and Deb 2011; Aminai pour 2012; Oreste  
138 2013; Chen et al. 2015; Changxing et al. 2015; Chang et al. 2017). However, many of  
139 the methods found and described in the literature, with all their advantages and  
140 limitations, are too complex to use for conventional design analysis. In particular, the  
141 analysis of the behaviour of passive bolts used to stabilise a potentially unstable rock  
142 block that slides along one or more surfaces is complex. In this case, the passive bolts  
143 were initially unloaded and even a slight movement (sometimes imperceptible) could  
144 activate them, causing forces to develop along their axes and forces to be transferred  
145 to the block capable of stabilising it.

146 This analysis can be done using numerical tools, but it requires rather long  
147 calculations and it is necessary to operate in a three-dimensional environment. An  
148 easier way to study the problem is to consider the bolt-rock interactions, both in the  
149 transverse and axial directions, using the Winkler spring approach (Oreste and  
150 Cravero, 2008; Oreste, 2009). In this way, the interaction phenomenon was studied in  
151 the elastic field and it was possible to quickly determine the stabilising forces of the  
152 bolt by evaluating the limits under the same operating conditions. Even this solution,  
153 however, requires a numerical solution to cope with the significant number of  
154 unknowns and the different boundary conditions that must be considered in order to

155 characterise the behaviour of the bolt. The analysis of the behaviour of passive bolts  
156 in a number of practical cases in which a bolt is needed to stabilise a block of  
157 potentially unstable rock and knowledge of the variability intervals of the parameters  
158 influencing the bolt-rock interaction allowed us to identify the critical points at which  
159 the bolt intersects with a lateral surface of the rock block.

160 In addition, some simplified hypotheses on the behaviour of the bolt with respect  
161 to the transverse interaction with the surrounding rock have produced negligible errors  
162 and can significantly simplify the mathematical model. In this paper, we review the  
163 fundamental equations that govern bolt-rock interactions using according to the  
164 independent Winkler springs approach. The development of the mathematical model  
165 is explained in order to achieve the stabilisation forces that the bolts apply to prevent  
166 a potentially unstable block from sliding along one or more surfaces that separate it  
167 from stable rock. The fundamental parameters influencing these stabilisation forces  
168 are analysed in order to speed up the design of the operations needed to stabilise a  
169 rock block with the necessary safety factors. A practical application to a real case  
170 allowed us to delineate the process of determining the influencing parameters and  
171 assessing the stabilisation forces as the diameter of the steel bar that constitutes the  
172 bolts varies.

### 173 **Mathematical development of the simplified approach**

174 Oreste and Cravero (2008) developed a mathematical procedure to calculate  
175 the stabilising forces applied by a passive bolt to a rock block and studied the effect of  
176 an axial displacement and a lateral displacement of the block with respect to the  
177 direction of the bolt axis. The direction of the displacement vector of the rock block  
178 was initially determined on the basis of the orientation of the sliding surface, in  
179 particular of the orientation of the line of intersection of the sliding surfaces.

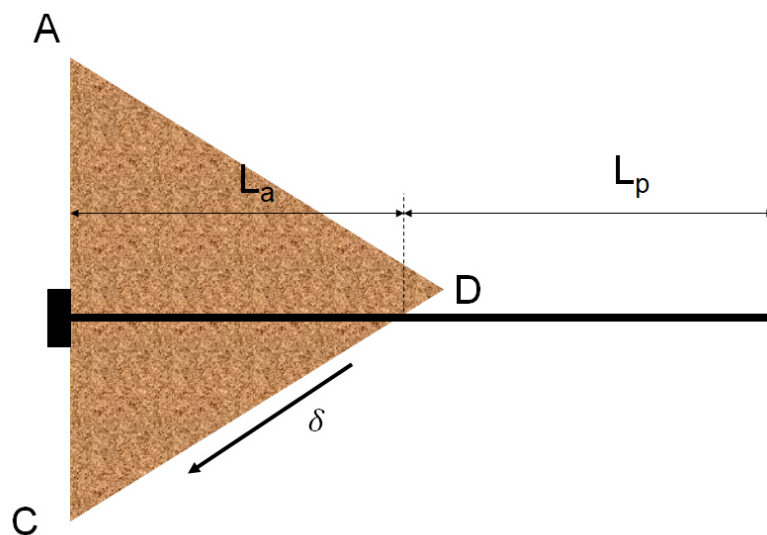
180 Then the angle  $\vartheta$ , which is the angle of the block displacement vector with the  
 181 direction of the axis of the passive bolts, was estimated (Oreste, 2009). In underground  
 182 applications, the bolts are generally arranged horizontally and perpendicular to the  
 183 cavity wall where there is a rock block which is potentially unstable due to sliding along  
 184 one or more natural discontinuities present in the rock mass.

185 The axial component,  $\delta_n$ , and the transversal component,  $\delta_t$ , of a generic  
 186 displacement of the rock block,  $\delta$ , are obtained from the following equations,  
 187 respectively:

$$188 \quad \delta_n = -\delta \cdot \cos(\vartheta) \quad (1)$$

$$189 \quad \delta_t = \delta \cdot \sin(\vartheta) \quad (2)$$

190 The effect of the axial component is to create a displacement of the block in the  
 191 direction of the bolt axis, with respect to the stable rock present at its contour. The  
 192 effect of the transversal component is to create a relative displacement of the block in  
 193 the direction perpendicular to the axis of the bolt, with respect to the stable rock  
 194 present at its contour (Fig. 2).



195  
 196 **Fig. 2 Schematic representation of the potentially unstable rock block and the**  
 197 **passive bolt (not to scale).  $L_a$  and  $L_p$  are the lengths of the bolt inside the**

198 **potentially unstable rock block (zone I) and in the stable rock (zone II),**  
 199 **respectively,  $\vartheta$  is the angle of the block displacement vector with the direction**  
 200 **of the axis of the passive bolts.**

201 From the analysis of the axial component of the displacement,  $\delta_n$ , it is possible  
 202 to obtain the trend of the axial force,  $N$ , along the bolt and the relative displacement  
 203  $v_r$  of the steel bar with respect to the surrounding rock and the shear stresses,  $\tau$ ,  
 204 developing at the interface between the bolt and the rock.

205 In more detail, the trend of the axial force  $N$  for the two areas in which the bolt  
 206 is divided were obtained from the following expressions:

207 Within the rock block (zone I):  $N = (EA)_{bolt} \cdot \alpha \cdot (H_{1,I} \cdot e^{\alpha x} - H_{2,I} \cdot e^{-\alpha x})$  (3)

208 In the stable rock (zone II):  $N = (EA)_{bolt} \cdot \alpha \cdot (H_{1,II} \cdot e^{\alpha x} - H_{2,II} \cdot e^{-\alpha x})$  (4)

209 Where:

210 
$$H_{1,I} = -\delta_n \cdot \frac{(1-e^{-2 \cdot \alpha \cdot L_p}) \cdot e^{-2 \cdot \alpha \cdot L_a}}{2 \cdot [1+e^{-2 \cdot \alpha \cdot (L_a+L_p)}]}$$
 (5)

211 
$$H_{2,I} = \delta_n \cdot \frac{(1-e^{-2 \cdot \alpha \cdot L_p})}{2 \cdot [1+e^{-2 \cdot \alpha \cdot (L_a+L_p)}]}$$
 (6)

212 
$$H_{1,II} = \delta_n \cdot \frac{(1+e^{-2 \cdot \alpha \cdot L_a}) \cdot e^{-2 \cdot \alpha \cdot L_p}}{2 \cdot [1+e^{-2 \cdot \alpha \cdot (L_a+L_p)}]}$$
 (7)

213 
$$H_{2,II} = \delta_n \cdot \frac{(1+e^{-2 \cdot \alpha \cdot L_a})}{2 \cdot [1+e^{-2 \cdot \alpha \cdot (L_a+L_p)}]}$$
 (8)

214  $L_a$  and  $L_p$  are the lengths of the bolt inside the potentially unstable rock block (zone I)  
 215 and in the stable rock (zone II), respectively, and their sum is the total length of the  
 216 bolt;  $\alpha$  is a parameter characterising the interaction in the axial direction between bolt  
 217 and rock as:

218 
$$\alpha = \sqrt{\frac{\beta_c \cdot P_{hole}}{(EA)_{bolt}}}$$
 (9)

219  $(EA)_{bolt}$  is the axial stiffness of the bolt, evaluated as:

220 
$$(EA)_{bolt} = E_{st} \cdot \left( \frac{\pi}{4} \cdot \Phi_{bar}^2 \right) + E_{binder} \cdot \left[ \frac{\pi}{4} \cdot (\Phi_{hole}^2 - \Phi_{bar}^2) \right] \quad (10)$$

221 **Where:**

222  $\Phi_{bar}$  is the bar diameter;

223  $E_{st}$  is the steel elastic modulus;

224  $E_{binder}$  is the elastic modulus of the binder surrounding the steel bar in the hole;

225  $P_{hole}$  is the perimeter of the cross-section of the bolt;

226  $\beta_c$  is the ratio between the shear stresses developing on the perimeter of the bolt (on

227 the wall of the hole),  $\tau$ , and the relative axial displacements,  $v_r$ .  $\beta_c$  depends in general

228 on the characteristics of the material surrounding the steel bar and on the elastic

229 modulus of the rock;

230  $\Phi_{hole}$  is the diameter of the hole where the bolt is inserted as  $\Phi_{hole} = \Phi_{bar} + 2 \cdot t_{binder}$ ;

231 and

232  $t_{binder}$  is the thickness of the binder annulus around the steel bar.

233 The distance  $x$ , measured along the bolt axis, originates at the intersection point of the

234 bolt with one of the block discontinuities (block surfaces). The shear stress,  $\tau$ , on the

235 lateral surface of the bolt is given by the following equations:

236 Within the rock block (zone I):  $\tau = -\beta_c \cdot (H_{1,I} \cdot e^{\alpha x} + H_{2,I} \cdot e^{-\alpha x}) \quad (11)$

237 In the stable rock (zone II):  $\tau = -\beta_c \cdot (H_{1,II} \cdot e^{\alpha x} + H_{2,II} \cdot e^{-\alpha x}) \quad (12)$

238 By analysing the transverse component of the displacement  $\delta_t$ , it is possible to

239 obtain the trend of the shear force  $T$  along the bolt, the transverse displacement of the

240 bolt  $y$  (in the direction perpendicular to its axis), and the bending moment  $M$ .

241 It has been noted by an extensive parametric analysis adopting input

242 parameters within ranges of variability typical of all possible cases which can be

243 encountered in practice that it is possible to adopt a simplified approach referring to

244 the hypothesis of infinite bolt length in the two considered zones (zone I and zone II)  
 245 making negligible errors (below 1%) (Oreste et al., 2020).

246 In more detail, the trend of the shear force  $T$ , according to this simplified approach,  
 247 was obtained from the following expression valid for both areas (zone I and II):

$$248 \quad T = (EJ)_{bolt} \cdot \beta^3 \cdot \delta_t \cdot e^{-\beta x} \cdot (\cos(\beta x) - \sin(\beta x)) \quad (13)$$

249 In the same way, the trend of the moment  $M$  along the bolt is given by the following  
 250 equation:

$$251 \quad M = (EJ)_{bolt} \cdot \beta^2 \cdot \delta_t \cdot e^{-\beta x} \cdot \sin(\beta x) \quad (14)$$

252 Where:

253  $(EJ)_{bolt}$  is the bending stiffness of the bolt, evaluated on the basis of the following  
 254 equation:

$$255 \quad (EJ)_{bolt} = E_{st} \cdot \left( \frac{\pi}{64} \cdot \Phi_{bar}^4 \right) + E_{binder} \cdot \left[ \frac{\pi}{64} (\Phi_{hole}^4 - \Phi_{bar}^4) \right] \quad (15)$$

256 and  $\beta$  is the parameter that characterises the interaction in the transverse direction  
 257 between bolt and rock:

$$258 \quad \beta = \sqrt[4]{\frac{k \cdot \Phi_{hole}}{4 \cdot (EJ)_{bolt}}} \quad (16)$$

259 where  $k$  is the ratio between the normal pressure,  $p$ , which is applied on the perimeter  
 260 of the bolt by the surrounding rock, and the transversal displacement,  $y$ , of the bolt.  
 261 The critical point along the bolt is identified at the intersection with a potentially  
 262 unstable rock block side surface ( $x = 0$ ). At that point, the stress state inside the bar  
 263 and on the bolt-rock interface is high. It is therefore useful to be able to evaluate the  
 264 stress characteristics of the forces  $N$  and  $T$ , and the shear stress value  $\tau$  for  $x = 0$ ,  
 265 considering that  $M_0$  ( $M$  for  $x=0$ ) is zero:

$$266 \quad N_0 = (EA)_{bolt} \cdot \alpha \cdot (H_{1,I} - H_{2,I}) \quad (17)$$

$$267 \quad T_0 = (EJ)_{bolt} \cdot \beta^3 \cdot \delta_t \quad (18)$$

268 
$$\tau_{0,I} = -\beta_c \cdot (H_{1,I} + H_{2,I}) \quad (19)$$

269 
$$\tau_{0,II} = -\beta_c \cdot (H_{1,II} + H_{2,II}) \quad (20)$$

270 From the previous equations it is possible to derive the safety factor of the bolt  
 271 with respect to the tensile failure of the steel bar ( $F_{s,yield}$ ) and to the failure of the bolt-  
 272 rock interface due to the bolt sliding ( $F_{s,slip}$ ):

273 
$$F_{s,yield} = \frac{\sigma_{yield}}{\sigma_{id}} \quad (21)$$

274 
$$F_{s,slip} = \frac{\tau_{lim}}{\tau_{0,II}} \quad (22)$$

275 Where:

276  $\sigma_{yield}$  is the yield stress of steel;

277  $\tau_{lim}$  is ultimate limit shear stress of the interface rock-bolt;

278  $\tau_{0,II}$  is the existing shear stress for  $x=0$  (at the intersection with a lateral surface of the  
 279 rock block) on the side of the portion of stable rock; this stress is greater than the  
 280 analogous stress existing on the side of the potentially unstable rock block ( $\tau_{0,I}$ ); and

281  $\sigma_{id}$  is the ideal stress which takes into account the simultaneous presence of an axial  
 282 and a shear stress in the section of the steel bar as expressed by:

283 
$$\sigma_{id} = \sqrt{\left(\frac{N_0}{A_{bar}}\right)^2 + 3 \cdot \left(\frac{T_0 \cdot S_{bar}}{\Phi_{bar} \cdot J_{bar}}\right)^2} \quad (23)$$

284 Where:

285  $A_{bar}$  is the area of the section of the steel bar constituting the bolt ( $A_{bar} = \pi \cdot \frac{\Phi_{bar}^2}{4}$ );

286  $S_{bar}$  is the static moment of the half section of the bar with respect to the barycentric

287 axis  $S_{bar} = \frac{1}{12} \cdot \Phi_{bar}^3$ ;

288  $J_{bar}$  is the moment of inertia of the steel bar constituting the bolt,  $J_{bar} = \pi \cdot \frac{\Phi_{bar}^4}{64}$ ;

289 By setting the values of the safety factors equal to the minimum values  
 290 considered admissible for the two failure mechanisms considered ( $F_{s,yield}=F_{s,adm,yield}$

291 and  $F_{s,slip} = F_{s,adm,slip}$ ) and by substituting, it is possible to obtain the following  
 292 equations of the maximum forces  $T_0$  and  $N_0$ . Referring to the failure of the steel bar at  
 293 the point of intersection with the block surface ( $x=0$ ):

$$294 \quad T_{0,max} = \frac{N_{yield}}{F_{s,adm,yield}} \cdot \frac{2}{\sqrt{\left[ \frac{(EA)_{bolt} \cdot \alpha}{(EJ)_{bolt} \cdot \beta^3} \right]^2 \cdot \left[ \frac{(1+e^{-2\alpha L_a}) \cdot (1-e^{-2\alpha L_p})}{(1+e^{-2\alpha(L_a+L_p)})} \right]^2 \cdot \frac{1}{\tan^2(\vartheta)} + \frac{64}{3}}} \quad (24)$$

$$295 \quad N_{0,max} = \frac{N_{yield}}{F_{s,adm,yield}} \cdot \frac{1}{\sqrt{1 + \frac{64}{3} \left[ \frac{(EJ)_{bolt} \cdot \beta^3}{(EA)_{bolt} \cdot \alpha} \right]^2 \cdot \left[ \frac{(1+e^{-2\alpha(L_a+L_p)})}{(1+e^{-2\alpha L_a}) \cdot (1-e^{-2\alpha L_p})} \right]^2 \cdot \tan^2(\vartheta)}} \quad (25)$$

296 Where:

297  $N_{yield}$  is the force causing bar failure under a tensile stress  $N_{yield} = \sigma_{yield} \cdot A_{bar}$ .

298 Referring to the failure of the bolt-rock interface at the point of intersection with  
 299 the surface of the block ( $x = 0$ ), with reference to the side on the stable rock, where  
 300 shear stress  $\tau$  is higher:

$$301 \quad T_{0,max} = 2 \cdot \frac{N_{slip}}{F_{s,adm,slip}} \cdot \left[ \frac{(EJ)_{bolt} \cdot \beta^3}{(EA)_{bolt} \cdot \alpha} \right] \cdot \left[ \frac{(1+e^{-2\alpha(L_a+L_p)})}{(1+e^{-2\alpha L_a}) \cdot (1+e^{-2\alpha L_p})} \right] \cdot \frac{1}{\alpha} \cdot \tan(\vartheta) \quad (26)$$

$$302 \quad N_{0,max} = \frac{N_{slip}}{F_{s,adm,slip}} \cdot \frac{1}{\alpha} \cdot \left[ \frac{(1-e^{-2\alpha L_p})}{(1+e^{-2\alpha L_p})} \right] \quad (27)$$

303 Where:

304  $N_{slip}$  is the force which causes the bolt-rock interface to fail for a unit bolt length  $N_{slip} =$   
 305  $\tau_{lim} \cdot \pi \cdot \Phi_{hole}$ .

306 The forces shown above represent the maximum forces that can be reached  
 307 when the safety factors of the bolt, in the two failure mechanisms considered, reach  
 308 the minimum allowable values. In practice, they are the maximum forces that can be  
 309 achieved with the movement of the rock block, while keeping the bolt in safe operating  
 310 condition. Verification against the two failure mechanisms must take place

311 simultaneously, and therefore, it was necessary to consider the minimum value  
 312 between the two pairs of forces:

$$313 \quad T_{0,max} = \min \left( \frac{N_{yield}}{F_{s,adm,yield}} \cdot \frac{2}{\sqrt{\frac{\lambda^2 \cdot \chi^2}{\tan^2(\vartheta)} + \frac{64}{3}}}; \frac{N_{slip}}{F_{s,adm,slip}} \cdot \frac{2 \cdot \tan(\vartheta)}{\lambda \cdot \psi \cdot \alpha} \right) \quad (28)$$

$$314 \quad N_{0,max} = \min \left( \frac{N_{yield}}{F_{s,adm,yield}} \cdot \frac{1}{\sqrt{1 + \frac{64}{3} \cdot \frac{\tan^2(\vartheta)}{\lambda^2 \cdot \chi^2}}}; \frac{N_{slip}}{F_{s,adm,slip}} \cdot \frac{\omega}{\alpha} \right) \quad (29)$$

315 Where:

$$316 \quad \lambda = \left[ \frac{(EA)_{bolt} \cdot \alpha}{(EJ)_{bolt} \cdot \beta^3} \right] \quad (30)$$

$$317 \quad \chi = \left[ \frac{(1+e^{-2\alpha L_a}) \cdot (1-e^{-2\alpha L_p})}{(1+e^{-2\alpha(L_a+L_p)})} \right] \quad (31)$$

$$318 \quad \psi = \left[ \frac{(1+e^{-2\alpha L_a}) \cdot (1+e^{-2\alpha L_p})}{(1+e^{-2\alpha(L_a+L_p)})} \right] \quad (32)$$

$$319 \quad \omega = \left[ \frac{(1-e^{-2\alpha L_p})}{(1+e^{-2\alpha L_p})} \right] \quad (33)$$

320

321 The forces obtained are of interest because they are the maximum values of  
 322 axial and shear forces that can be achieved along the bolt (in particular at the point of  
 323 intersection of the bolt with a lateral surface of the block). They also represent the  
 324 stabilising forces that the single bolt applies to the potentially unstable rock block in  
 325 the direction of the bolt axis ( $N_{0,max}$ ) and in the transverse direction (perpendicular to  
 326 the bolt axis). This plane includes the block displacement vector (i.e., the intersection  
 327 line of the sliding surfaces) and the bolt axis ( $T_{0,max}$ ).

### 328 Analysis of the stabilising forces of the passive bolt

329 The stabilisation forces were evaluated starting from the limit forces  $N_{yield}$  and  
 330  $N_{slip}$  (which caused the two failure mechanisms described above) and the respective

331 minimum safety factors considered acceptable. It is also necessary to know the angle  
 332 that the displacement vector of the block forms with the axis of the bolt ( $\vartheta$ ) and the  
 333 stiffness parameters  $\lambda$  and  $\alpha$ . Other parameters that link the stiffness parameters to  
 334 the geometric ones ( $L_a$  and  $L_p$ ) are necessary for the calculation of  $\chi$ ,  $\psi$ , and  $\omega$ .

335 **Figures 3 through 9 show graphs of the dimensionless parameters  $\lambda$ ,  $\chi$ ,  $\psi$ , and**  
 336  **$\omega$  with changing stiffness value  $\alpha$  for different bar diameters  $\Phi_{bar}$ ,  $L_a$ , and  $L_p$  and for**  
 337 **the stiffness parameter  $\beta$ . The values of bolt length and diameter adopted in the**  
 338 **mathematical model are assumed on the basis of values available in the literature**  
 339 **(e.g., Bawden, 2011; DSI, 2015).**

340 **The graphs were obtained considering  $t_{binder}$  equal to 10 mm,  $E_{steel}$  equal to**  
 341 **210 GPa, and  $E_{binder}$  equal to 25 GPa. From the analysis of the figures, it is possible**  
 342 **to detect how for  $\alpha > 5$ , the parameters  $\chi$  and  $\psi$  can be set equal to 1; and the**  
 343 **parameter  $\omega$  can be set equal to 1 for  $\alpha > 2$ . In all other cases, it is necessary to**  
 344 **calculate the values through equations 30–33) or by using the graphs in Figures 3–6;**  
 345 **then to proceed with the evaluation of the maximum forces  $T_{0,max}$  and  $N_{0,max}$**   
 346 **mobilisable by each bolt (eq. 28 and 29). If  $\alpha > 5$ , then equations 28 and 29 simplify**  
 347 **as follows:**

$$348 \quad T_{0,max} = \min\left(\frac{N_{yield}}{F_{s,adm,yield}} \cdot \xi; \frac{N_{slip}}{F_{s,adm,slip}} \cdot \frac{\eta}{\alpha}\right) \quad (34)$$

$$349 \quad N_{0,max} = \min\left(\frac{N_{yield}}{F_{s,adm,yield}} \cdot \varrho; \frac{N_{slip}}{F_{s,adm,slip}} \cdot \frac{1}{\alpha}\right) \quad (35)$$

350 Where:

$$351 \quad \xi = \frac{2}{\sqrt{\frac{\lambda^2}{\tan^2(\vartheta) + 3} + 64}} \quad (36)$$

$$352 \quad \eta = \frac{2 \cdot \tan(\vartheta)}{\lambda} \quad (37)$$

353

$$\varrho = \frac{1}{\sqrt{1 + \frac{64 \tan^2(\vartheta)}{3 \lambda^2}}} \quad (38)$$

354

355

356

357

358

For these cases, the length values  $L_a$  and  $L_p$  do not longer influence the values of the stabilising forces. The path of  $\xi$ ,  $\eta$ , and  $\varrho$  as functions of  $\lambda$  and the angle  $\vartheta$  are shown in Figures 7–9. The obtained forces ( $T_{0,max}$  and  $N_{0,max}$ ) can then be included in the analyses for the block stability and therefore, to design the bolting intervention necessary to achieve stabilisation of the block.

359

360

361

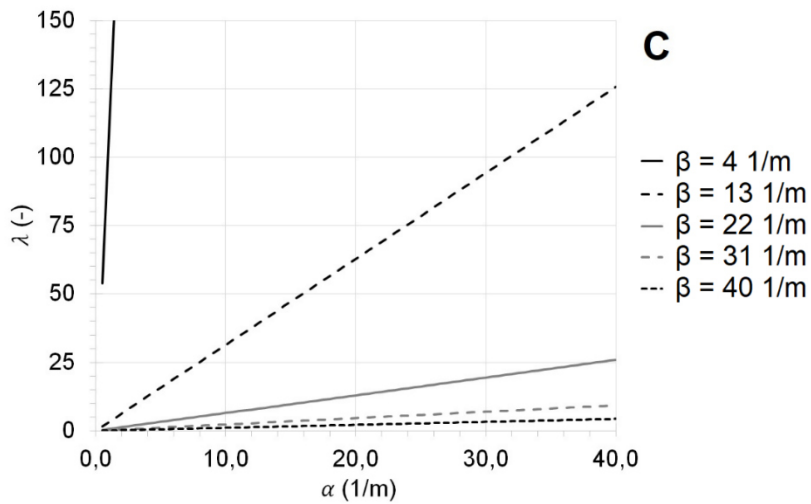
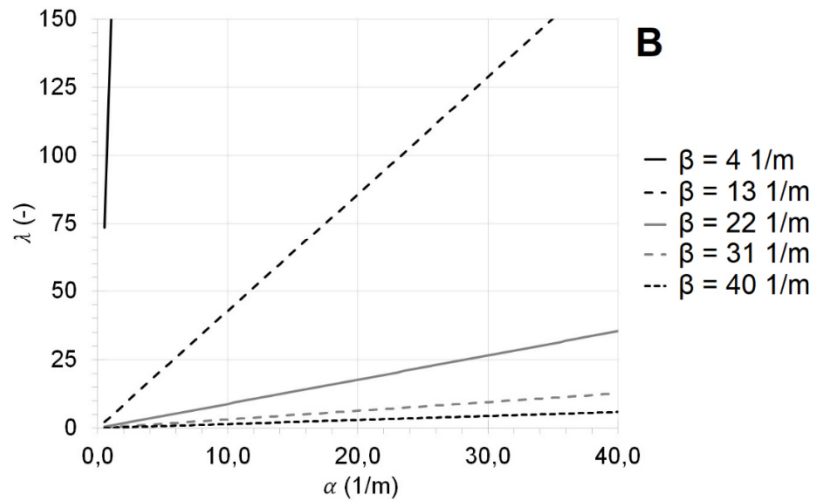
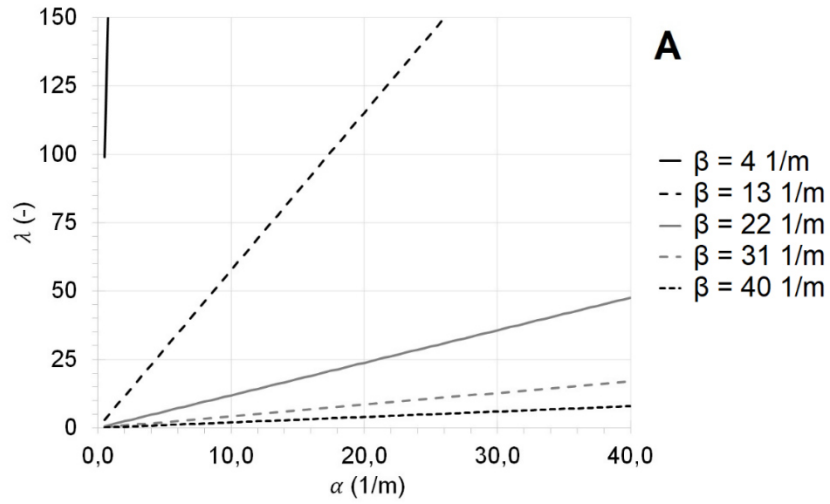
362

363

364

365

All the parameters mentioned in equations 30–33 and 36–38 are dimensionless and are only useful to better understand the evolution of the coefficients  $T_{0,max}$  and  $N_{0,max}$  by varying some fundamental parameters in the rock-bolt interaction. The only parameter that has an important physical meaning is  $\lambda$  (eq. 30), which is the ratio between the product of the stiffness parameters referred to the axial interaction divided by the product of the stiffness parameters referred to the transverse interaction between bolt and rock.

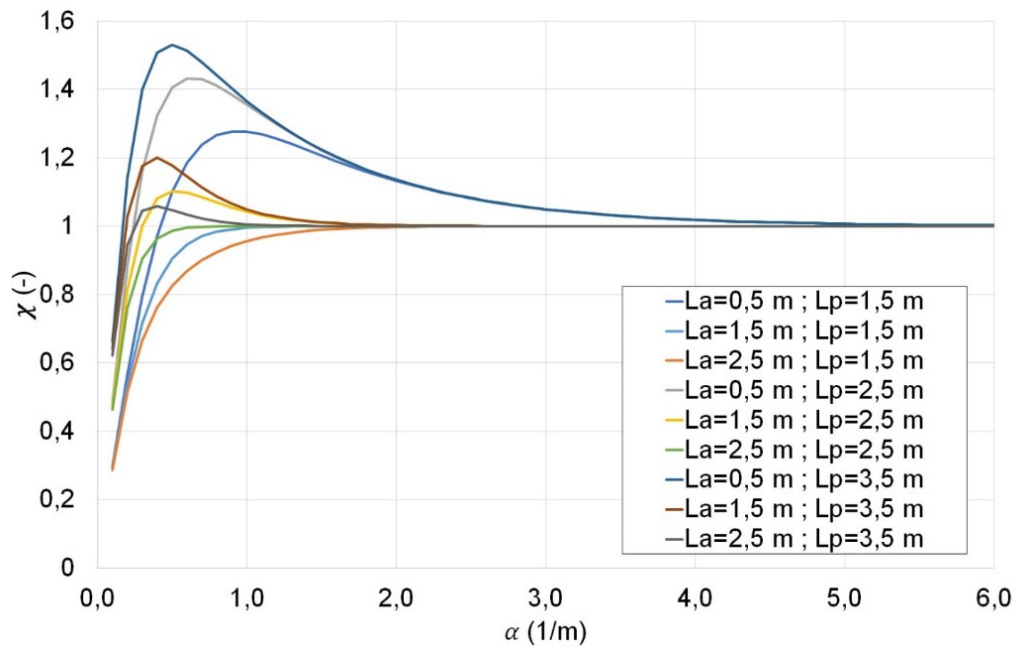


366

367 **Fig. 3 Trend of the parameter  $\lambda$  by changing  $\alpha$  for different values of  $\beta$ . A) Bar**

368 **diameter 20 mm; B) Bar diameter 28 mm; C) Bar diameter 36 mm.**

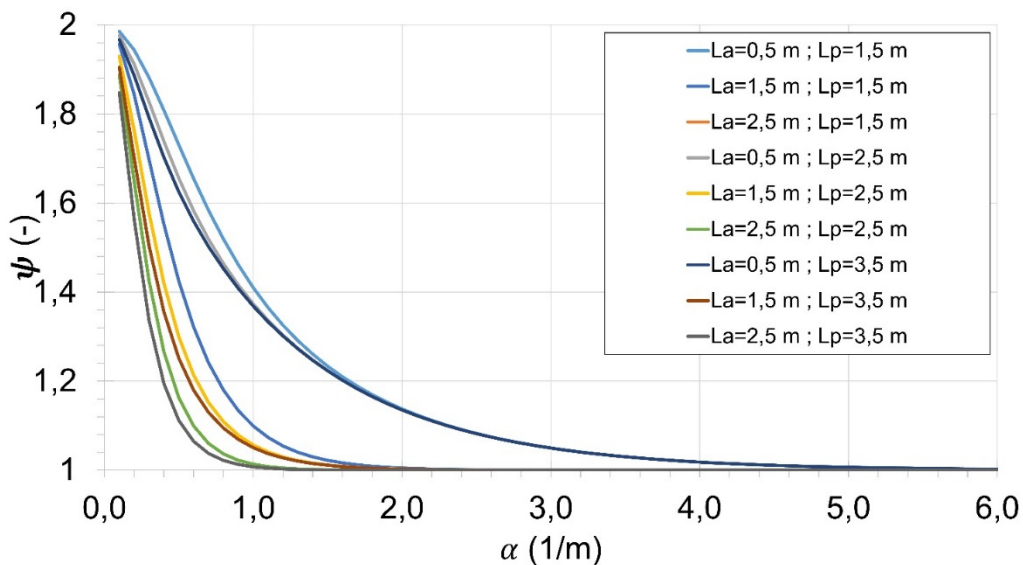
369



370

371 **Fig. 4 Trend of the parameter  $\chi$  by changing  $\alpha$  for different values of  $L_a$  (bolt**  
 372 **section in the potentially unstable rock block) and  $L_p$  (bolt section in stable**  
 373 **rock).**

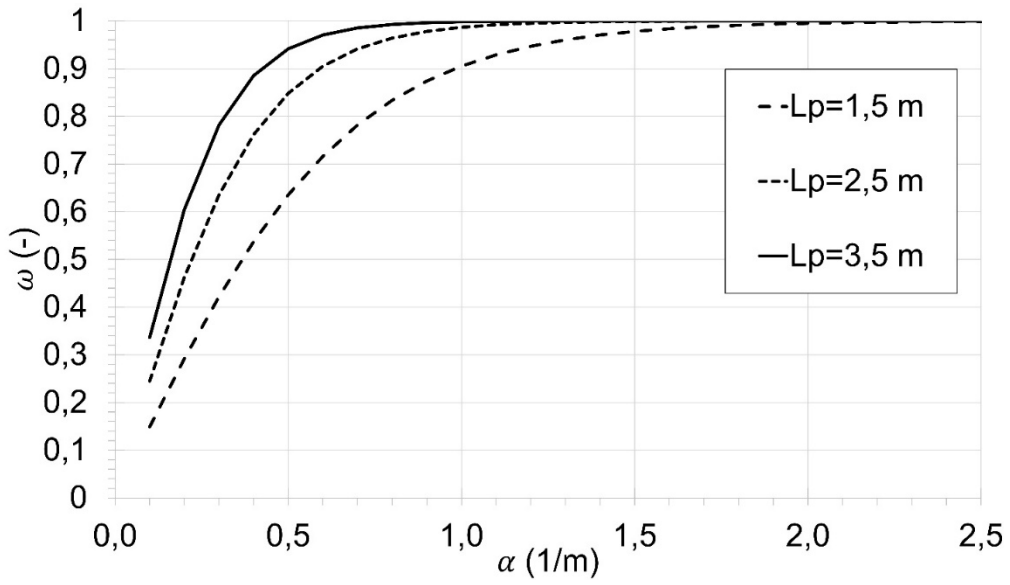
374



375

376 **Fig. 5 Trend of parameter  $\psi$  by changing  $\alpha$  for different values of  $L_a$  (bolt section**  
 377 **in the potentially unstable rock block) and  $L_p$  (bolt section in stable rock). The**  
 378 **line with  $L_a=1.5$  m and  $L_p=2.5$  m overlaps the line with  $L_a=2.5$  m and  $L_p=1.5$  m.**

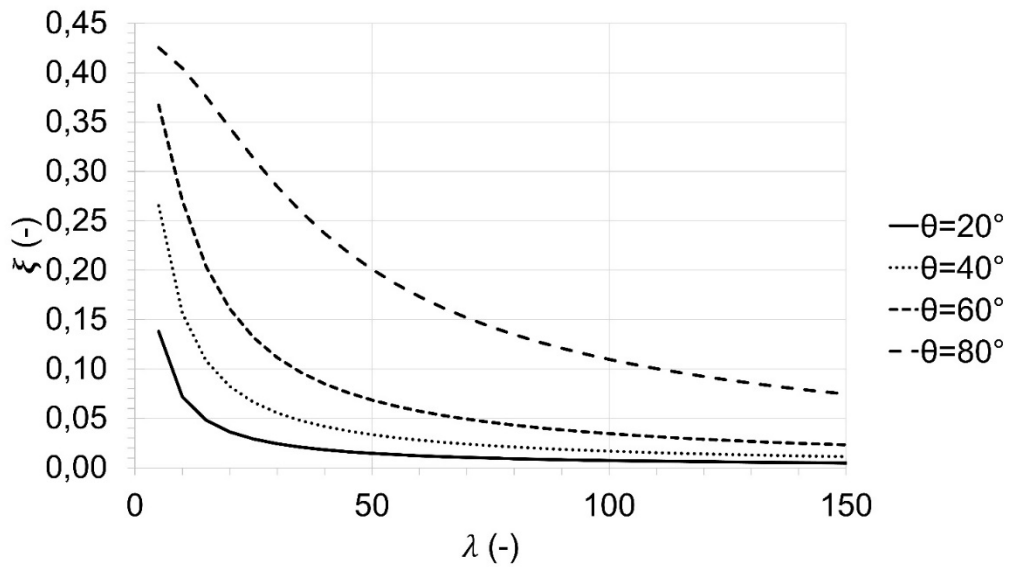
379



380

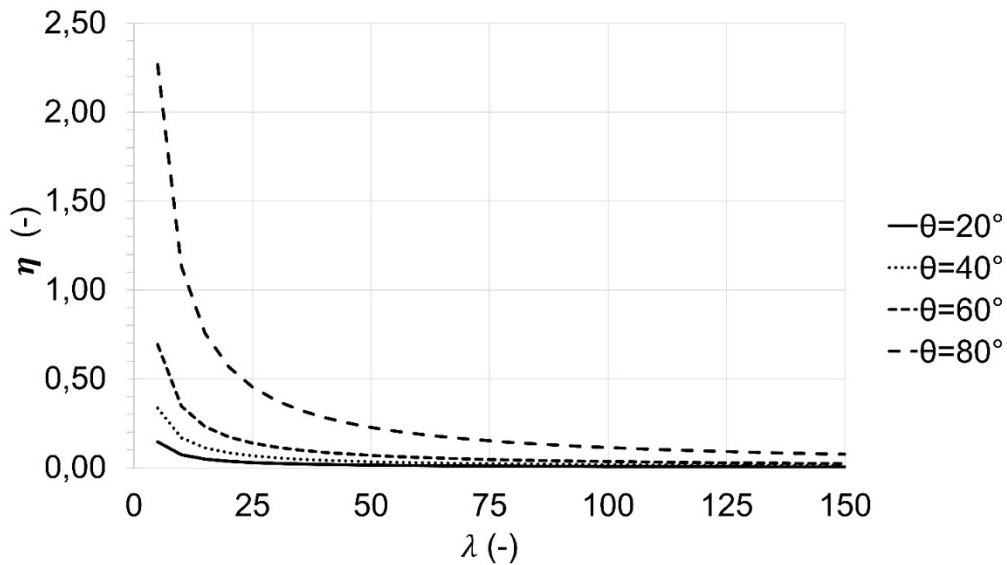
381 **Fig. 6 Trend of the parameter  $\omega$  for  $L_a=0.5$  m (bolt section in the potentially**  
382 **unstable rock block) and different values of  $L_p$  (bolt section in stable rock).**

383



384

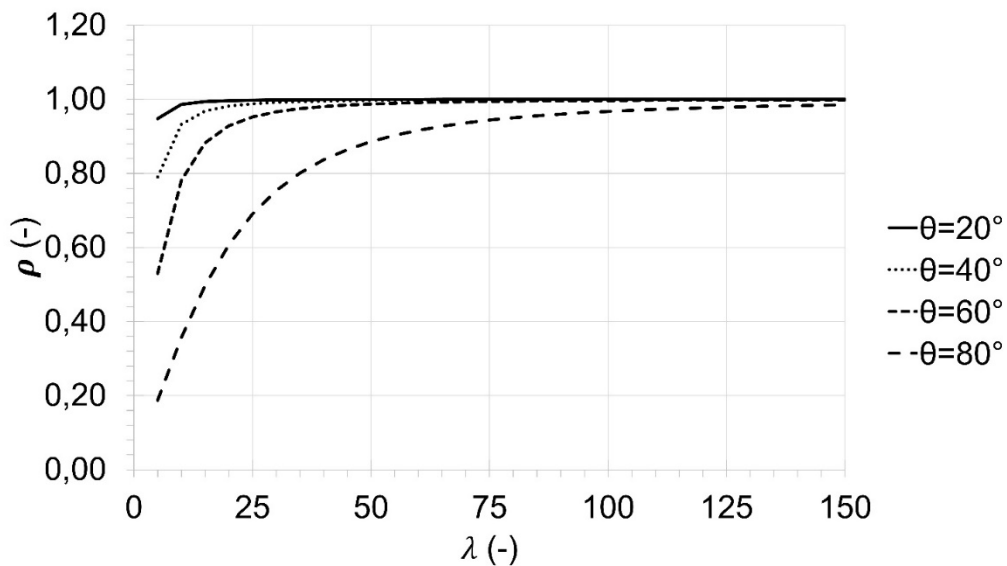
385 **Fig. 7 Trend of the parameter  $\xi$  by varying  $\lambda$  for different values of angle  $\vartheta$ .**



386

387 **Fig. 8 Trend of the parameter  $\eta$  by varying  $\lambda$  for different values of angle  $\vartheta$ .**

388



389

390 **Fig. 9 Trend of the parameter  $\rho$  by varying  $\lambda$  for different values of angle  $\vartheta$ .**

391 **Application of the theoretical equations to a real case**

392 Based on the theoretical model discussed above, the importance of the stiffness  
 393 parameters of the bolt-rock interaction ( $\alpha$  and  $\beta$ ) on the behaviour of passive bolts is  
 394 evident (see eq. 9 and 16). These parameters, which have the inverse dimension of  
 395 length, depend respectively on the axial  $(EA)_{bolt}$  (eq. 10) and bending stiffness

396  $(EJ)_{bolt}$  (eq. 15) of the bolt and on the parameters  $k$  and  $\beta_c$ . The parameter  $k$   
397 represents the ratio between the normal contact pressure,  $p$ , on the external surface  
398 of the bolt and the lateral displacement,  $y$ , of the bolt in the direction perpendicular to  
399 its axis ( $p = k \cdot y$ ). On the other hand,  $\beta_c$  represents the ratio between the shear stress  
400  $\tau$  developing on the lateral surface of the bolt and the bolt-rock relative displacement  
401  $v_r$  in the axial direction ( $\tau = \beta_c \cdot v_r$ ). The parameters  $k$  and  $\beta_c$  can be obtained from  
402 specific in situ tests on bolts of reduced length (even the diameter may be different  
403 from what is intended to be used for the stabilisation of the block). More specifically,  $k$   
404 can be obtained from lateral shear tests by applying a force perpendicular to the axis  
405 of the bolt in correspondence to its head ( $T_{test}$ ), while  $\beta_c$  is obtained from pull-out tests  
406 of the bolt with the application of a tensile axial force at the bolt head ( $N_{test}$ ).

407 The stabilising force equations  $N_{0,max}$  and  $T_{0,max}$  (eq. 28 and 29) have been  
408 applied to the case of a potentially unstable rock block in a limestone formation (mean  
409 intact UCS values were about 140 MPa) present near a municipal road in Northern  
410 Piedmont (Northern Italy). The block had a planar sliding surface with an inclination of  
411  $35^\circ$  with respect to the horizontal plane. The cement was CEM I 52.5 R with a  
412 water/cement ratio,  $w/c$ , 0.45, which is typical of anchors in rock (e.g., Littlejohn and  
413 Bruce, 1977). The grout was cured for 28 days prior to testing. Transverse load tests  
414 and pull-out tests were performed.

415 The transverse load test (a non-destructive test) was carried out first, until a  
416 force compatible with the elastic behaviour of the bolt and its interface with the  
417 surrounding rock was reached. In the transverse load test (Fig. 10), a concrete ballast  
418 was connected to the bolt head through a rope. A dynamometric device applied stress  
419 on the rope and thus applied the test force ( $T_{test}$ ) to the bolt head. The force was  
420 increased in equal intervals until the maximum test force was reached. For each value

421 of the applied force, the displacement of the head  $\delta_{t,test}$  was measured in the same  
422 direction as the force through high precision strain gauges. It was possible to plot a  
423 diagram of  $T_{test}$  vs.  $\delta_{t,test}$ , which identified a straight line that best approximated the  
424 experimental points, and to evaluate the angular coefficient which represents the ratio  
425  $T_{test}/\delta_{t,test}$ . This ratio is useful for estimating the stiffness parameter  $k$  (eq. 39) and the  
426 stiffness parameter  $\beta$  (eq. 16). In the specific case examined, the transverse load test  
427 reached the maximum force of 0.75 tons with four successive load steps of equal  
428 value; the final displacement was 0.4 mm. The angular coefficient of the interpolated  
429 straight line was found to be approximately 18.4 MN/m. It was taken as the  $T_{test}/\delta_{t,test}$   
430 (eq. 39), from which the value of the stiffness parameter,  $k$ , in the transverse  
431 interaction bolt-rock was estimated. The ratio between the applied force and the  
432 measured lateral displacement allowed us to obtain the parameter  $k$  from the following  
433 equation:

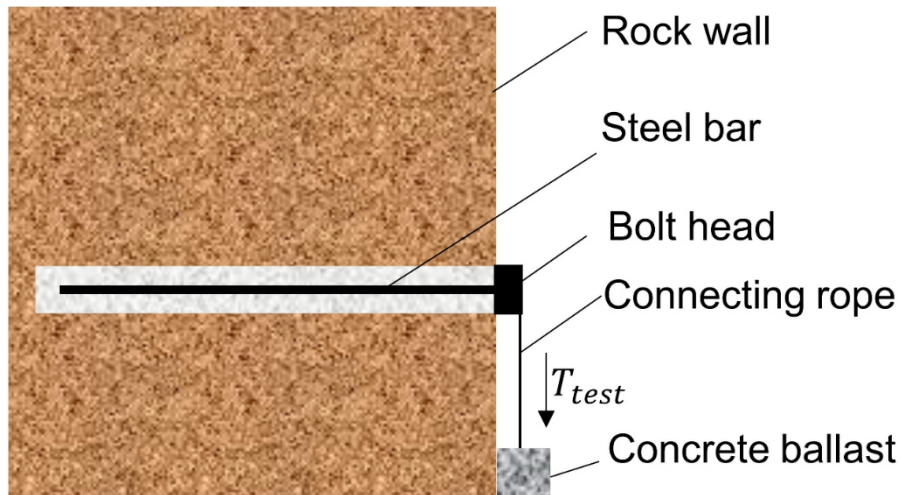
$$434 \quad k = \frac{\sqrt[3]{4}}{\Phi_{hole,test} \sqrt[3]{(EJ)_{bolt,test}}} \cdot \left( \frac{T_{test}}{\delta_{t,test}} \right)^{\frac{4}{3}} \quad (39)$$

435 Where:

436  $\delta_{t,test}$  is the lateral bolt head displacement due to the application of a lateral shear  
437 force,  $T_{test}$ ;

438  $\Phi_{hole,test}$  is the diameter of the tested bolt; and

439  $(EJ)_{bolt,test}$  is the bending stiffness of the tested bolt.



440

441 **Fig. 10 Sketch of the transverse load test for the evaluation of the stiffness**  
 442 **parameters  $k$  and  $\beta$  (not to scale).**

443 After the lateral test, a strain-controlled pull-out test was performed to obtain  
 444 the relation  $N_{,test} - \delta_{n,test}$ , applying a 0.3 mm/sec pull rate. The test continued until the  
 445 bolt was removed (i.e., failure of the bolt-rock interface) to evaluate the limit shear  
 446 stress,  $\tau_{lim}$ , on the lateral surface of the bolt:

447 
$$\tau_{lim} = \frac{N_{slip,test}}{\pi \cdot \Phi_{hole,test} \cdot L_{test}} \quad (40)$$

448 Where:

449  $N_{slip,test}$  is the force which causes the bolt-rock interface of the test bolt to fail (i.e. bolt  
 450 slips away).

451 By carrying out bolt pull-out tests, it was possible to evaluate  $\beta_c$  as a function of the  
 452 ratio between the applied axial force and the measured axial displacement (Oreste  
 453 and Cravero, 2008):

454 
$$\beta_c = \frac{1}{P_{hole,test} \cdot (EA)_{bolt,test} \cdot \tanh^2 \left( \sqrt{\frac{\beta_c \cdot P_{hole,test}}{(EA)_{bolt,test}} \cdot L_{test}} \right)} \cdot \left( \frac{N_{test}}{\delta_{n,test}} \right)^2 \quad (41)$$

455 Where:

456  $L_{test}$  is the length of the tested bolt;

457  $\delta_{n,test}$  is the bolt head axial displacement due to the application of the axial force,  $N_{test}$ ;

458  $P_{hole,test}$  is the perimeter of the tested bolt; and

459  $(EA)_{bolt,test}$  is the axial stiffness of the tested bolt.

460 Given the form of the equation, a numerical solution was then carried out.

461 Experimental tests on a test bolt of 0.75 m length with a bar of 24 mm diameter  
462 and a thickness of the cementitious binder,  $t_{binder}$ , equal to 10 mm provided the  
463 following values:

- 464 • average lateral displacement  $\delta_{t,test}$  of about 0.4 mm in the presence of a lateral  
465 force  $T_{test}$  of 0.75 tons;
- 466 • average axial displacement  $\delta_{n,test}$  of about 0.1 mm in the presence of an axial  
467 force  $N_{test}$  of 1 ton; and
- 468 • a pull-out force  $N_{slip,test}$  of 22 tons.

469 From the tests carried out it was possible to obtain the parameters  $k$  (8.9  
470 MPa/mm),  $\beta_c$  (1.18 MPa/mm), and  $\tau_{lim}$  (2.08 MPa). From these values, the remaining  
471 parameters necessary for the calculations were obtained for the different diameters of  
472 the steel bar, assuming  $L_a = 1.5$  m (bolt length inside the block) and  $L_p = 2.5$  m  
473 (anchoring length in the stable rock):

474  $\Phi_{bar}=20$  mm:  $\alpha = 1.5966$ ;  $\beta = 11.7975$ ;  $\lambda = 12.31$ ;  $\chi = 1.00797$ ;  $\psi = 1.008655$ ;  $\omega = 0.99932$ ;

475  $\Phi_{bar}=24$  mm:  $\alpha = 1.3954$ ;  $\beta = 10.6492$ ;  $\lambda = 12.71$ ;  $\chi = 1.01424$ ;  $\psi = 1.016135$ ;  $\omega = 0.99813$ ;

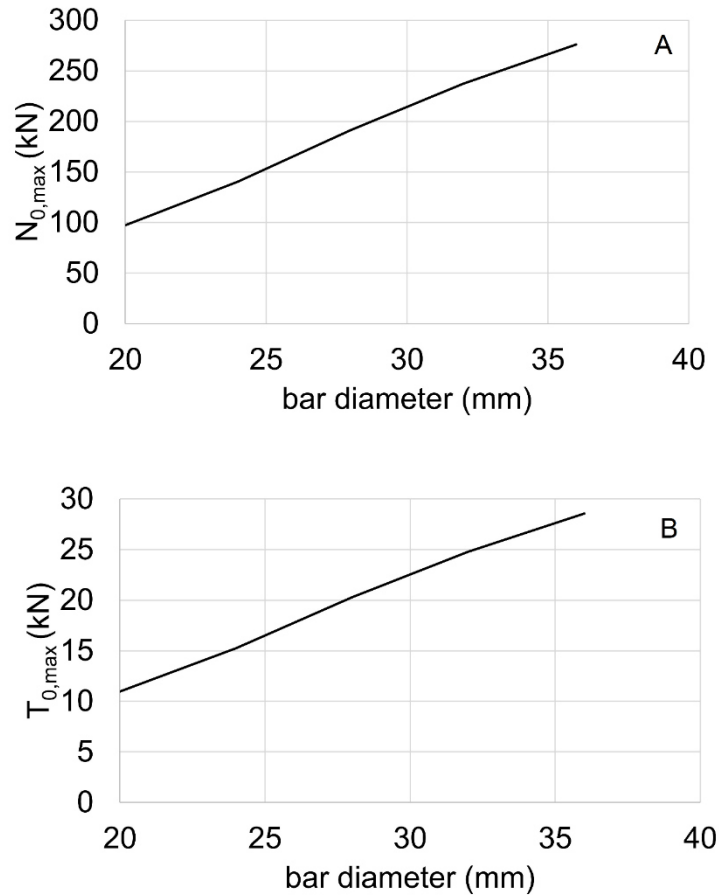
476  $\Phi_{bar}=28$  mm:  $\alpha = 1.2492$ ;  $\beta = 9.6936$ ;  $\lambda = 12.93$ ;  $\chi = 1.02154$ ;  $\psi = 1.025507$ ;  $\omega = 0.99613$ ;

477  $\Phi_{bar}=32$  mm:  $\alpha = 1.1377$ ;  $\beta = 8.8935$ ;  $\lambda = 13.02$ ;  $\chi = 1.02933$ ;  $\psi = 1.036320$ ;  $\omega = 0.99325$ ;

478  $\Phi_{bar}=36$  mm:  $\alpha = 1.0494$ ;  $\beta = 8.2178$ ;  $\lambda = 13.05$ ;  $\chi = 1.03720$ ;  $\psi = 1.048177$ ;  $\omega = 0.98953$ .

479

480 Finally, using equations 28 and 29, with  $\sigma_{yield} = 400$  MPa and  $F_{s,adm,yield} =$   
 481  $F_{s,adm,slip} = 1.25$ , we obtained the trend of stabilising forces shown in Fig. 11A and  
 482 11B.  
 483



484  
 485 **Fig. 11 Trend of the axial stabilisation force ( $N_{0,max}$ ) (A) and of the transverse**  
 486 **stabilisation force  $T_{0,max}$  (B) as the diameter of the steel bar varies for the case**  
 487 **study.**

488 Knowing the stabilising forces that each bolt is able to offer to the potentially  
 489 unstable rock block, it is possible to design the bolting system (number and diameter  
 490 of the bolts) needed to achieve the desired safety factor with regard to the block sliding.

491 **Conclusions**

492 The analysis of the behaviour of a passive bolt used to stabilise a potentially unstable  
493 rock block from sliding along one or more surfaces is complex and requires three-  
494 dimensional numerical modelling in the presence of specific interfaces that represent  
495 the discontinuity surfaces that isolate the block and the contact surfaces of the bolt  
496 from the surrounding rock. Using the Winkler springs approach to simulate the bolt-  
497 rock interaction in the transverse and axial directions, a numerical solution was created  
498 in order to manage the numerous unknowns in the problem.

499 Thanks to the identification of specific critical points during the operation of  
500 passive bolts (at the point of intersection with the lateral surface of the block) and to  
501 the knowledge of the variability of intervals typical of the influential parameters that  
502 characterise the bolt-rock interaction, it was possible to develop a mathematical model  
503 to obtain the two stabilising forces that the bolt applies to the potentially unstable block.  
504 This model was based on some simplified hypotheses that produce a negligible error  
505 thanks to an extensive parametric analysis that considers intervals of variability typical  
506 of the parameters influencing the problem. These stabilisation forces are, in fact, the  
507 forces that must be considered as the static contribution of the bolt to reach conditions  
508 **stable enough to be deemed** acceptable for the potentially unstable block. One force  
509 was directed in the axial direction of the bolt; the other in a direction perpendicular to  
510 the axis of the bolt and lying in the plane which included the axis of the bolt and the  
511 displacement vector of the rock block.

512 **The equations obtained allowed us to quickly evaluate the extent of the**  
513 **stabilising forces as a function of the diameter of the steel bar and therefore made it**  
514 **possible to correctly design the bolting operation by defining the bolt diameter and the**  
515 **number of bolts needed to stabilise the block of rock. An example from a real case**

516 allowed us to apply the equations obtained and chart the trend of the stabilisation  
517 forces as the diameter of the bar constituting the bolt changed.

## 518 **Conflict of interests**

519 Authors declare they have no conflict of interest.

## 520 **References**

- 521 1. Aminai pour, F., 2012. The effect load transfer mechanism of fully grouted bolts,  
522 M.Sc Thesis, Department of mine, Islamic Azad University, Bafgh, Iran.
- 523 2. Aziz, N., Jalalifar, H., 2007. The role of profile configuration on load transfer  
524 mechanism of bolt for effective support. J. Mines Met. Fuels (Dec), 539–545.
- 525 3. Bawden, F.W. (2011). Ground Control Using Cable and Rock Bolting. In:  
526 Darling, P., Ed., SME Mining Engineering Handbook, Society for Mining,  
527 Metallurgy and Exploration Inc., Littleton, 616-617.
- 528 4. Blümel, M., Schweiger, H.F., Golser, H., 1997. Effect of rib geometry on the  
529 mechanical behavior of grouted rock bolts. World Tunneling Congress'97. In:  
530 23rd General Assembly of the International Tunneling Association, Wien, pp.  
531 6–7.
- 532 5. Changxing, Z., Xu, C., Youdong, M., Xulin, L. (2015). Modeling of grout crack  
533 of rockbolt grouted system. International Journal of Mining Science and  
534 Technology 25, 73–77.
- 535 6. Chang, X., Wang,G., Liang, Z., Yang, J., Tang C. (2017). Study on grout  
536 cracking and interface debonding of rockbolt grouted system. Construction and  
537 Building Materials 135, 665–673

- 538 7. Chappell, B.A., 1989. Rock bolts and shear stiffness in jointed rock mass. J.  
539 Geotech. Eng. 115, 2, 179-197, [https://doi.org/10.1061/\(ASCE\)0733-](https://doi.org/10.1061/(ASCE)0733-9410(1989)115:2(179))  
540 [9410\(1989\)115:2\(179\)](https://doi.org/10.1061/(ASCE)0733-9410(1989)115:2(179)).
- 541 8. Chen, J., Saydam, S., Hagan, P.C. (2015). An analytical model of the load  
542 transfer behavior of fully grouted cable bolts. Construction and Building  
543 Materials 101, 1006–1015.
- 544 9. Das, K., Deb, D., 2011. Analytical model for fully grouted rock bolts considering  
545 movements of rock joints. Third Indian Rock Conference by ISRM-TT, 187–199.
- 546 10. DSI, 2015. Mechanical Anchors and Rebar Rock Bolts,  
547 [https://static1.squarespace.com/static/529f28d4e4b0cf8c82ff287b/t/52acf49be](https://static1.squarespace.com/static/529f28d4e4b0cf8c82ff287b/t/52acf49be4b0e46ab625d265/1387066523589/DSI-ALWAG-Systems_Mechanical-Anchors-and-Rebar-Rock-Bolts.pdf)  
548 [4b0e46ab625d265/1387066523589/DSI-ALWAG-Systems\\_Mechanical-](https://static1.squarespace.com/static/529f28d4e4b0cf8c82ff287b/t/52acf49be4b0e46ab625d265/1387066523589/DSI-ALWAG-Systems_Mechanical-Anchors-and-Rebar-Rock-Bolts.pdf)  
549 [Anchors-and-Rebar-Rock-Bolts.pdf](https://static1.squarespace.com/static/529f28d4e4b0cf8c82ff287b/t/52acf49be4b0e46ab625d265/1387066523589/DSI-ALWAG-Systems_Mechanical-Anchors-and-Rebar-Rock-Bolts.pdf), last access December 1, 2021.
- 550 11. Ferrero, M. (1995). The shear strength of reinforced rock joints. International  
551 Journal of Rock Mechanics and Mining Sciences & Geomechanics Abstracts,  
552 32, 6, 595-605.
- 553 12. Ghadimi, M., Shahriar, K., Jalalifar, H. (2015). Tunnelling and Underground  
554 Space Technology, 50, 143-151.
- 555 13. Lancellotta, R., and Cavalera, J. (1999) Fondazioni. Mc Graw Hill, Milano
- 556 14. Lang TA (1961) Theory and practice of rock bolting. Trans Soc Min Engrs Am  
557 Inst Min Metall Petrolm Engrs 220: 333–348.
- 558 15. Li, C.C. (2017). Principles of rockbolting design. Journal of Rock Mechanics  
559 and Geotechnical Engineering. 9, 396-414.
- 560 16. Littlejohn, G.S., Bruce, D.A. (1977). Rock Anchors-State of the Art. Foundation  
561 Publications Ltd. Brentwood, UK.

- 562 17. Nie, W., Zhao, Z.Y., Ning, Y.J., and Guo, W. (2014). Numerical studies on  
563 rockbolts mechanism using 2D discontinuous deformation analysis. *Tunnelling  
564 and Underground Space Technology*, 41, 223–233.
- 565 18. Oreste, P.P., and Cravero, M. (2008). An analysis of the action of dowels on  
566 the stabilization of rock blocks on underground excavation walls. *Rock  
567 Mechanics and Rock Engineering*, 41(6), 835–868, DOI 10.1007/s00603-008-  
568 0162-2.
- 569 19. Oreste PP, Dias D (2012) Stabilisation of the excavation face in shallow tunnels  
570 using fibreglass dowels. *Rock Mechanics Rock Eng.*, 45(4): 499-517. DOI:  
571 10.1007/s00603-012-0234-1
- 572 20. Oreste, P.P. (2009). Face stabilisation of shallow tunnels using fibreglass  
573 dowels. *Proceedings of the Institution of Civil Engineers-Geotechnical  
574 Engineering*, 162, GE2, 95–109, doi: 10.1680/geng.2009.162.2.95.
- 575 21. Oreste, P (2013). Face stabilization of deep tunnels using longitudinal  
576 fibreglass dowels. *International Journal of Rock Mechanics and Mining  
577 Sciences*, 58, 127-140, <https://doi.org/10.1016/j.ijrmms.2012.07.011>.
- 578 22. Oreste, P., Spagnoli, G., Buccoleri, A.G. (2020). A parametric analysis on the  
579 influence of the binder characteristics on the behaviour of passive rock bolts  
580 with the Block Reinforcement Procedure. *Geotechnical and Geological  
581 Engineering*, <https://doi.org/10.1007/s10706-020-01285-7>.
- 582 23. Osgoui, R.R., Oreste P. (2007). Convergence-control approach for rock tunnels  
583 reinforced by grouted bolts, using the homogenization concept. *Geotechnical  
584 and Geological Engineering*, 25, 431–440, [https://doi.org/10.1007/s10706-007-  
585 9120-0](https://doi.org/10.1007/s10706-007-9120-0).

- 586 24. Ranjbarnia, M., Fahimifar, A., Oreste, P. (2014). A simplified model to study the  
587 behavior of pre-tensioned fully grouted bolts around tunnels and to analyze the  
588 more important influencing parameters. *Journal of Mining Science*, 50 (3), 533-  
589 548.
- 590 25. Ranjbarnia M, Fahimifar A, Oreste P (2016) Practical Method for the Design of  
591 Pretensioned Fully Grouted Rockbolts in Tunnels. *Int J Geomech* 16(1):  
592 [https://doi.org/10.1061/\(ASCE\)GM.1943-5622.0000464](https://doi.org/10.1061/(ASCE)GM.1943-5622.0000464).
- 593

594 **FIGURE CAPTION**

595 Fig. 1 Sketch of a passive rock bolt.

596 Fig. 2 Schematic representation of the potentially unstable rock block and the passive  
597 bolt (not to scale).  $L_a$  and  $L_p$  are the lengths of the bolt inside the potentially unstable  
598 rock block (zone I) and in the stable rock (zone II), respectively,  $\vartheta$  is the angle of the  
599 block displacement vector with the direction of the axis of the passive bolts.

600 Fig. 3 Trend of the parameter  $\lambda$  by changing  $\alpha$  for different values of  $\beta$ . A) Bar diameter  
601 20 mm; B) Bar diameter 28 mm; C) Bar diameter 36 mm.

602 Fig. 4 Trend of the parameter  $\chi$  by changing  $\alpha$  for different values of  $L_a$  (bolt section  
603 in the potentially unstable rock block) and  $L_p$  (bolt section in stable rock).

604 Fig. 5 Trend of parameter  $\psi$  by changing  $\alpha$  for different values of  $L_a$  (bolt section in  
605 the potentially unstable rock block) and  $L_p$  (bolt section in stable rock). The line with  
606  $L_a=1.5$  m and  $L_p=2.5$  m overlaps the line with  $L_a=2.5$  m and  $L_p=1.5$  m.

607 Fig. 6 Trend of the parameter  $\omega$  for  $L_a=0.5$  m (bolt section in the potentially unstable  
608 rock block) and different values of  $L_p$  (bolt section in stable rock).

609 Fig. 7 Trend of the parameter  $\xi$  by varying  $\lambda$  for different values of angle  $\vartheta$ .

610 Fig. 8 Trend of the parameter  $\eta$  by varying  $\lambda$  for different values of angle  $\vartheta$ .

611 Fig. 9 Trend of the parameter  $\rho$  by varying  $\lambda$  for different values of angle  $\vartheta$ .

612 Fig. 10 Sketch of the transverse load test for the evaluation of the stiffness parameters  
613  $k$  and  $\beta$  (not to scale).

614 Fig. 11 Trend of the axial stabilisation force ( $N_{0,max}$ ) (A) and of the transverse  
615 stabilisation force  $T_{0,max}$  (B) as the diameter of the steel bar varies for the case study.